

# EXPERIMENTAL STUDY AND DYNAMIC THERMAL MODELING OF SOLID SENSIBLE HEAT STORAGE SYSTEM

K. Vigneshwaran<sup>1</sup>, Gurpreet Singh Sodhi<sup>2</sup>, P. Muthukumar<sup>1,2,\*</sup>, Anurag Guha<sup>3</sup>, S. Senthilmurugan<sup>1,3</sup>

<sup>1</sup>Centre for Energy, Indian Institute of Technology Guwahati, Guwahati, India – 781039

<sup>2\*</sup>Department of Mechanical Engineering, Indian Institute of Technology Guwahati, Guwahati, India – 781039

<sup>3</sup>Department of Chemical Engineering, Indian Institute of Technology Guwahati, Guwahati, India – 781039

## ABSTRACT

In the present study, the thermal behavior of the high-temperature Concrete based Thermal Energy Storage (CTES) system is investigated using experimental study and simplified 1D dynamic modeling. The storage module is made up of shell and tube configuration. The shell side is filled with concrete as the energy storage material, and air is circulated in the tube (made of copper) side. The operating temperature range of the storage module is fixed in between 170 and 240 °C. The 1D dynamic modeling is developed using a set of equations, which helps to predict the heat transfer characteristics of the CTES module. In addition, the overall performance of the CTES module is investigated by integrating the developed model with real-time solar collector data and the seed dryer model. It is observed that, during the off-sun hours, the CTES module is capable of generating the hot air for the continuous drying of grape seed.

**Keywords:** Sensible heat storage; Concrete; Experimental validation; Thermal modelling; Solar thermal application

## NOMENCLATURE

<i>Abbreviations</i>	
CTES	Concrete Thermal Energy Storage
HTF	Heat Transfer Fluid
SHS	Sensible Heat Storage
<i>Symbols</i>	
$A$	area (m <sup>2</sup> )
$c_p$	specific heat (J/kg-K)
$D$	diameter of storage module (m)
$d$	diameter of HTF tube (m)
$k$	thermal conductivity (W/m-K)
$M$	molecular weight of air (kg/mol)
$m$	mass (kg)

$n$	number of HTF tubes
$Nu$	nusselt number
$P$	air pressure (N/m <sup>2</sup> )
$q$	heat transfer rate (W/m <sup>2</sup> )
$T$	temperature (°C)
$t$	time (s)
$U_o$	overall heat transfer coefficient (W/m <sup>2</sup> -K)
$V$	volume (m <sup>3</sup> )
$v$	velocity (m/s)
$X$	moisture content (%)(dry basis-d.b)
$\rho$	density (kg/m <sup>3</sup> )
$\mu$	viscosity (Ns/m <sup>2</sup> )
$\varepsilon$	porosity
$\psi$	mass transfer rate per unit area (g/m <sup>2</sup> -s)
<i>Subscripts</i>	
$avg$	average
$c$	concrete
$d$	dryer
$s$	seed

## 1. INTRODUCTION

Solar energy technology plays an important role in reducing the CO<sub>2</sub> emission. However, due to the intermittent nature of solar energy, a continuous supply of energy is not possible, which can be addressed by Thermal Energy Storage (TES). In TES, solid Sensible Heat Storage (SHS) system is a promising technology which provides a high-quality heat for longer life cycle with negligible degradation in material quality [1]. Few researchers have studied the performance of concrete as the TES material. As compared to the other solid SHS material, the heat capacity of concrete is high, and it is

also easily available and cheaper. Also, concrete is highly durable up to 500 °C, and it can withstand multiple charging and discharging cycles without any crack or deformation. John et al. [2] have studied the degradation of concrete from ambient to 500 °C. They concluded that 75 % of the compressive strength was retained without any crack after ten thermal cycles. However, during the first charging cycle, some studies were indicated the formation of minor cracks on the concrete module. The crack formation is rectified by introducing a polytetrafluoroethylene layer coating at the periphery of the Heat Transfer Fluid (HTF) tube. Air is selected as the HTF, due to its corrosion-resistance property and wide operating temperature range. In recent times, various studies have been discussed about the integration of TES with applications such as space heating, process heat, drying, concentrated solar power, etc.

To overcome the difficulties existing in 3D models such as high computational time and infrastructure, some researchers have attempted to study the performance of TES system using 1-D dynamic modeling which helps in real-time monitoring and optimization of the application. Geissbühler et al. [3] have developed a dynamic model for maintaining the constant outlet temperature from TES using materials such as rock and encapsulated AlSi<sub>12</sub>. It is observed that most of the reported literature on sensible heat storage system are mainly focused on the study of TES material degradation, exploration of alternative materials and improvement of material properties. It is also observed from the literature that there is a lack of studies on the design and experimentation of high-temperature concrete based thermal energy storage of the cylindrical multi-tube system. Therefore, the major objective of the current manuscript is to investigate the thermal behavior of the high-temperature concrete based sensible heat storage system using air as the heat transfer fluid. Based on the experiments performed, the 1-D dynamic model is developed to study the performance of the CTES system by integrating with real-time solar collector and dryer model.

## 2. EXPERIMENTAL PROCEDURE

### 2.1 System description

The experiment facility consists of a CTES module, a centrifugal blower and an air heater. The centrifugal blower is used to blow the air to the CTES module through a heating element. Air velocity is controlled by using a variable frequency drive, and air temperature is controlled by using the air heater's heating element on/off controller. The CTES module is made of shell and

tube configuration. The shell side is filled with concrete mixture, and the air is circulated through the tube side, as illustrated in Fig. 1. K-Type thermocouples are placed along module length and radius (25/50/75 mm radius from the outer periphery and 40/500/960 mm length from entrance) for measuring the CTES module temperature. Based on the previous study conducted by the author's team on optimization of the number of tubes [4], twenty-two HTF tubes (made of copper) are embedded inside the concrete, and each tube has five copper fins brazed on the outer periphery to enhance the heat transfer rate. The length and diameter of CTES are 1000 mm and 324 mm, whereas the HTF tube has outer diameter and thickness of 12.7 mm and 1.5 mm, respectively. Thickness and height of the fin are 2 mm and 10 mm, respectively.

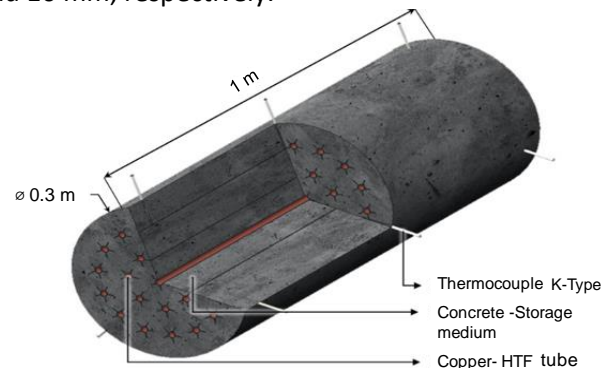


Fig 1. 3-dimensional view of the CTES module.

During the charging process, the CTES module was heated from 170 to 240 °C and vice versa during the discharging. During charging and discharging processes, the Inlet temperature of the air was maintained at 300 °C and 130 °C, respectively. The module is said to be fully charged or discharged once the volume average temperature of the storage module reaches the steady-state value. The velocity of the air was maintained at 9.9 m/s at the inlet of the HTF tube. The maximum uncertainty in the measurement of flow rate was  $\pm 3.33\%$  ( $\pm 0.0492$  kg/min).

### 2.2 Modeling of CTES module with application

From the experimental study, it was observed that there was less temperature variation in the radial direction in comparison with the axial direction of the CTES module. Therefore, the ID model for CTES is developed by connecting three numbers of lumped system models in the series. This ID model is indented to predict the module and HTF temperature variation across the module length. Then, the module heat storage capacity can be calculated by using the average module temperature.

In single lumped CTES element, for both charging or discharging condition, the air is passed through HTF tubes to either deliver or absorb the heat. The heat and mass balance equation for the HTF is given below:

$$nV_{t,i} \frac{d(\rho_{air} c_{p,air} T_{air})_{out}}{dt} = A_t n ((v_{air} \rho_{air} c_{p,air} T_{air})_{in} - (v_{air} \rho_{air} c_{p,air} T_{air})_{out}) - q \quad (1)$$

$$nV_{t,i} \frac{d(\rho_{air,out})}{dt} = nA_{t,i} ((v_{air} \rho_{air})_{in} - (v_{air} \rho_{air})_{out}) \quad (2)$$

The rate of heat transfer between the CTES and air are;

$$q = \frac{U_{overall} n A_{sur} (\Delta T_{in} - \Delta T_{out})}{\ln \left( \frac{\Delta T_{in}}{\Delta T_{out}} \right)} \quad (3)$$

where,  $\Delta T$  represents the temperature difference between the CTES module and the air. The average temperature of the CTES module is calculated using Eq. (4).

$$q = \frac{dT_{c,avg}}{dt} m_c c_{p,c} \quad (4)$$

The heat energy stored or discharged is given as:

$$Q(t) = V_c \rho_c c_{p,c} (T_{c,avg}(t) - T_{ini}) \quad (5)$$

The Hagen-Poiseuille and ideal gas equations are used to calculate the pressure drop and density of air across the CTES module and are described as:

$$\frac{P_{air,out} - P_{air,in}}{L} = \left( \frac{128}{\pi} \right) \left( \frac{\mu_{air,avg}}{d_{t,i}^4} \right) (vA_t) \quad (6)$$

$$\rho_{air} = \frac{PM}{RT_{air}} \quad (7)$$

The Dittus-Boelter equation is used to estimate the Nusselt number, where 'a' and 'b' are 0.023 and 0.8. 'c' = 0.4 for heating and 0.3 for cooling.

$$Nu = a Re^b Pr^c \quad (8)$$

The values of 'c', 'b' and 'a' can be estimated using the temperature values obtained from experimental results. Using the design library of Dymola, it is possible to minimize the error between the experiments and the predicted data using the following error function;

$$\text{Error}(t) = \sum_{t=1}^t \left[ \sqrt{\left( 1 - \frac{(T_{c,avg}(t))_{\text{model}}}{(T_{c,avg}(t))_{\text{Experiment}}} \right)^2} + \sqrt{\left( 1 - \frac{(T_{air,out}(t))_{\text{model}}}{(T_{air,out}(t))_{\text{Experiment}}} \right)^2} \right] \quad (9)$$

The overall heat transfer coefficient is estimated using Eq. (10). Based on these model equations, the model can

predict the thermal behavior of the CTES module. As shown in Fig. 2, the upstream side of the developed CTES model is integrated with the solar collector output temperature reported by Lakshmi et al. [5]. The downstream process of the CTES module is coupled with the grape seed dryer model adopted from the literature [6]. The moisture removal rate of seed dryer is estimated with and without CTES module.

$$U_{overall} = \left[ \left( \frac{d_{t,o}}{h_t d_{t,i}} \right) + \left( \frac{d_{t,o} \ln \left[ \frac{d_{t,o}}{d_{t,i}} \right]}{k_p 2} \right) \right]^{-1} + \left( \frac{d_{t,o} \ln \left[ \frac{D_{c,avg}}{d_{t,o}} \right]}{k_c 2} \right) \quad (10)$$

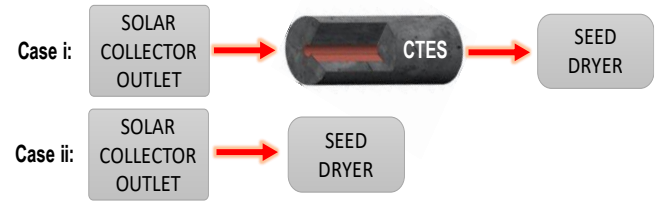


Fig 2. Schematic diagram of the seed dryer with (Case i) and without (Case ii) the CTES module.

The mass balance across the seeds is described as:

$$V_d \rho_s (1 - \varepsilon) \frac{dX}{dt} = -\psi_s A_d \quad (5)$$

The energy balance concerning the dryer section:

$$L_s (\psi_s A_d) + \rho_s \frac{dV_d (1 - \varepsilon) c_{p,s} T_s}{dt} = h_t A_d \frac{(T_{air,in} - T_s) - (T_{air,out} - T_s)}{\log \left( \frac{T_{air,in} - T_s}{T_{air,out} - T_s} \right)} \quad (6)$$

### 3. RESULT AND DISCUSSIONS

The results obtained from the 1-D dynamic model are validated using the experimental results for both the charging and discharging processes. During validation of both the processes, the initial and inlet conditions are maintained as mentioned in Section 2.1. From Fig. 3 (a) and (b), it can be observed that the results of the experiments and model are having a close match with a maximum error of  $\pm 4.9^\circ\text{C}$ .

The performance of the solar dryer integrated with CTES module is simulated using a flowsheet model developed in this study. From author's team reported data [5], the variation in the intensity of the solar radiation in a day and the corresponding outlet temperature of air from the solar collector are used to simulate the CTES application. This data has been

reported for the solar conditions on the day of 19<sup>th</sup> March 2016 at Bhubaneswar, India. Further, the corresponding solar collector outlet temperature, as shown in Fig. 4 (as per Case-i, Fig. 2) is given as an input to the CTES module.

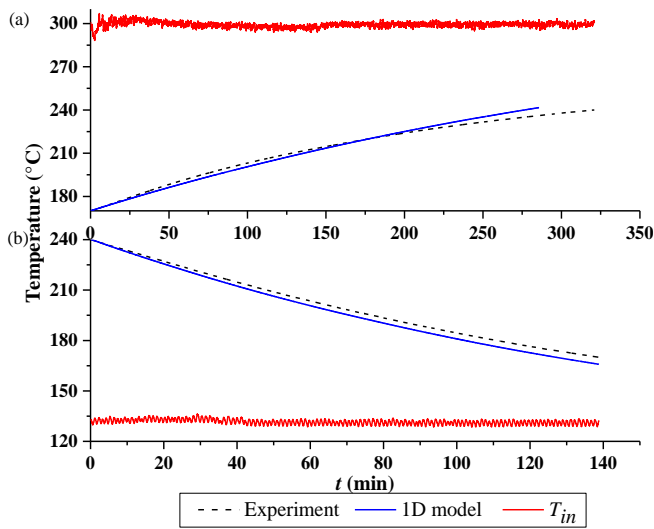


Fig 3. Validation of the 1D model with experiment (a) charging process, (b) discharging process.

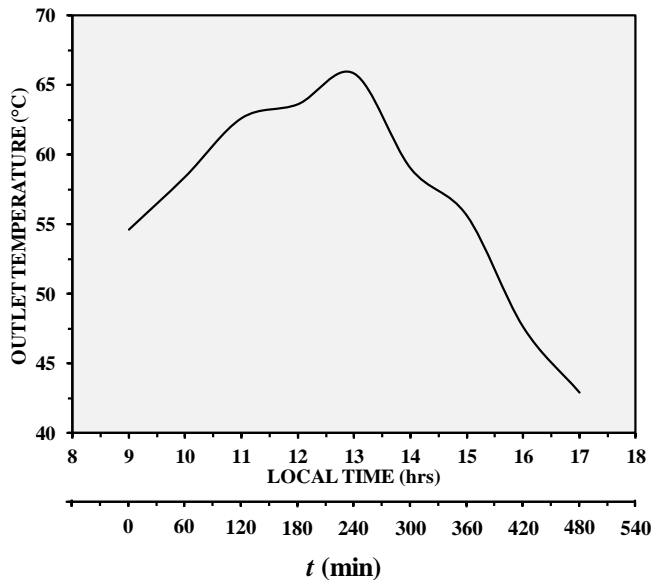


Fig 4. Outlet temperature of solar collector adopted from Lakshmi et al.[5].

The CTES module is operated with an initial temperature of 65 °C and depending upon the variation in solar radiation (or outlet temperature of solar collector), the module is subjected to either discharging or charging processes. The heat transfer between the air and CTES module depends upon the temperature of the air entering into the CTES module. When air inlet temperature of CTES module is less than volume average

temperature of the CTES module, the module is discharged, whereas, when air inlet temperature of CTES module is higher than volume average temperature of the CTES module, the module is charged. Hence, there is a varying temperature profile at the air outlet of the CTES module, which is governed by an air inlet temperature of the CTES module proportional to the solar intensity. The variation in the air outlet temperature and net CTES energy stored/discharged are presented in Fig. 5.

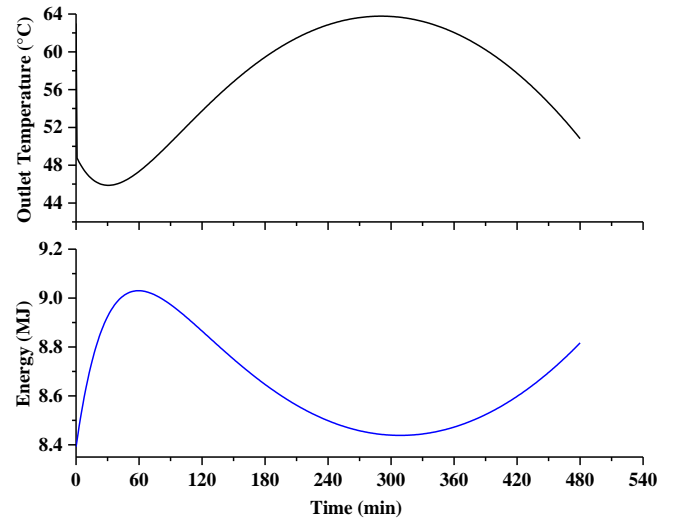


Fig 5. Thermal behavior of the CTES module with respect to solar collector output (for Case i - with CTES module).

During real-time operation, directly supplying the outlet condition of solar collector will affect the structure of seed. Therefore, while integrating the CTES module in the loop, moisture removal rate from the seed will become steady, and it may help to retain the medicinal values of the dried seed [7].

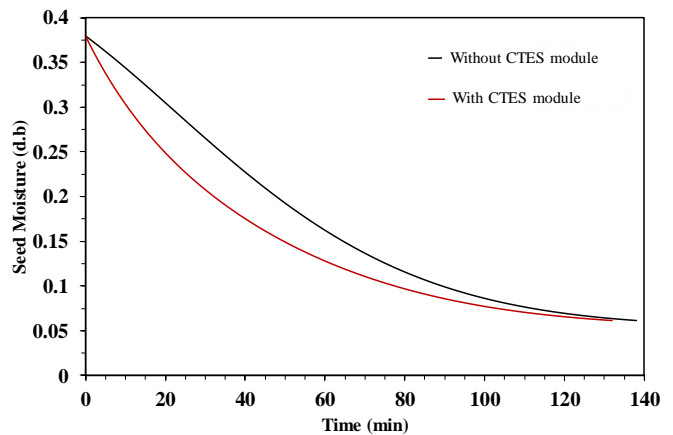


Fig 6. Performance of seed dryer (moisture removal rate from seed) with and without CTES module.

The output air from the CTES module is supplied to the seed dryer at initial moisture content of 37% (dry

basis) and temperature of 25 °C. The humidity ratio and velocity of air at the inlet of the dryer are 0.019 kg/kg and 1.6 m/s, respectively. Fig. 6 shows the performance of the dryer with (as per Case-i, Fig. 2) and without (as per Case-ii, Fig. 2) the CTES module. As observed from results obtained, the performance of the dryer is much more superior while operating in Case-i as compared to Case-ii.

#### 4. CONCLUSION

The thermal behavior of the concrete based thermal energy storage system made of cylindrical multi-tube configuration is analysed using the experiments and simplified 1D dynamic modeling. The results of the dynamic model are having good agreement with the experimental data. Later, the possibility of integrating the solar thermal application with CTES is explored by coupling the developed model with solar collector and seed dryer. The moisture removal rate from seed is analysed with and without the CTES module. It is observed that the CTES module helps to remove the moisture at a faster and uniform rate even during the off-sun period.

#### ACKNOWLEDGEMENT

The authors would like to thank the Department of Science and Technology (DST), Government of India, for their financial support (Project No: DST/TMD/SERUD12(C)).

#### REFERENCE

- [1] K. Vigneshwaran, G.S. Sodhi, P. Muthukumar, A. Guha, S. Senthilmurugan, Experimental and numerical investigations on high temperature cast steel based sensible heat storage system, *Appl. Energy*. 251 (2019) 113322. doi:10.1016/j.apenergy.2019.113322.
- [2] E.E. John, W.M. Hale, R.P. Selvam, Development of a High-Performance Concrete to Store Thermal Energy for Concentrating Solar Power Plants, in: *ASME 2011 5th Int. Conf. Energy Sustain. Parts A, B, C*, ASME, Washington, DC, USA, 2011: pp. 523–529. doi:10.1115/ES2011-54177.
- [3] L. Geissbühler, M. Kolman, G. Zanganeh, A. Haselbacher, A. Steinfeld, Analysis of industrial-scale high-temperature combined sensible/latent thermal energy storage, *Appl. Therm. Eng.* 101 (2016) 657–668. doi:10.1016/j.applthermaleng.2015.12.031.
- [4] L. Prasad, P. Muthukumar, Design and optimization of lab-scale sensible heat storage prototype for solar thermal power plant application, *Sol. Energy*. 97 (2013) 217–229. doi:10.1016/j.solener.2013.08.022.
- [5] D.V.N. Lakshmi, A. Layek, P.M. Kumar, Performance Analysis of Trapezoidal Corrugated Solar Air Heater with Sensible Heat Storage Material, *Energy Procedia*. 109 (2017) 463–470. doi:10.1016/j.egypro.2017.03.069.
- [6] G. Johann, E.A. da Silva, N.C. Pereira, Modelling and optimisation of grape seed drying: Equivalence between the lumped and distributed parameter models, *Biosyst. Eng.* 176 (2018) 26–35. doi:10.1016/j.biosystemseng.2018.10.004.
- [7] D.V.N. Lakshmi, P. Muthukumar, A. Layek, P.K. Nayak, Drying kinetics and quality analysis of black turmeric (*Curcuma caesia*) drying in a mixed mode forced convection solar dryer integrated with thermal energy storage, *Renew. Energy*. 120 (2018) 23–34. doi:10.1016/j.renene.2017.12.053.